Industrial byproducts for the soil stabilization of trace elements and per- and polyfluorinated alkyl substances (PFASs)

Yaxin Zhang [a,b], Gerard Cornelissen [b,c], Ludovica Silvani [c], Valentina Zivanovic [b], Andreas Botnen Smebye [c], Erlend Sørmo [b,c], Gorm Thune [d], Gudny Okkenhaug [b,c,*]

[a] College of Environmental Science and Engineering, Hunan University, Lushan Gate, Lushan South Road, Yuelu District, Changsha 100084, China
[b] Norwegian University of Life Sciences (NMBU), Faculty of Environmental Sciences and Natural Resource Management, PB 5003 NMBU, Ås 1432, Norway
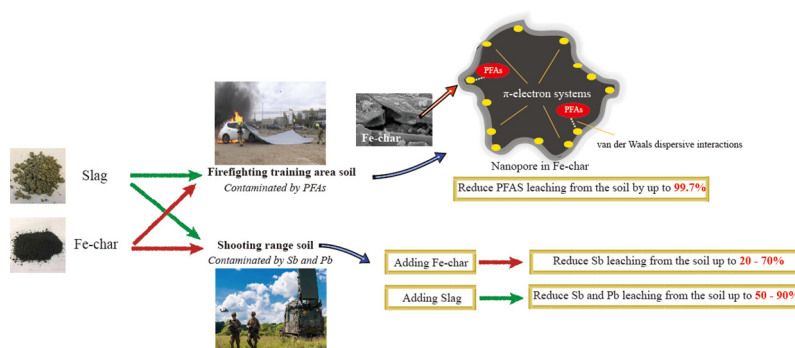[c] Norwegian Geotechnical Institute (NGI), Department of Environmental Engineering, PB 3930 Ullevaal Stadion, 0806 Oslo, Norway
[d] Lindum AS, Lerpeveien 155, Drammen, Norway

HIGHLIGHTS

- Two ubiquitous industrial by-products from titanium and iron processing were applied as soil pollution sorbents.
- The remediation effectiveness of the adsorbent materials on PFAS, Pb, and Sb in various kinds of soils was investigated.
- A detailed physicochemical characterization of the adsorbents was done to elucidate adsorption mechanisms.
- Both industrial by-products proved to be promising soil remediation materials.

GRAPHICAL ABSTRACT

ABSTRACT

The present work was the first exploration of the use of industrial byproducts from iron and titanium processing as sorbents for the stabilization of soil contamination. The main aim was to test slag waste and iron-rich charred fossil coal ("Fe-char"), as sorbents for *per*- and polyfluorinated alkyl substances (PFASs), as well as lead (Pb) and antimony (Sb), in four soils from a firefighting training area (PFASs) and a shooting range (Pb and Sb).

Adding slag (10–20%) to shooting range soils decreased the leaching of Pb and Sb up to 50–90%. Fe-char amendment to these soils resulted in a moderate reduction in Sb leaching (20–70%) and a slightly stronger effect on Pb (40–50%). The sorption is most likely explained by the presence of Fe oxyhydroxides. These are present in the highest concentrations in the slag, probably resulting in more effective metal binding to the slag than to the Fe-char.

Fe-char but not slag proved to be a strong sorbent for PFASs (reducing PFAS leaching from the soil by up to 99.7%) in soil containing low total organic carbon (TOC; 1.2%) but not in high-TOC soil (34%). The sorption coefficient K_D for Fe-char was high, in the range of $10^{4.3}$ to $10^{6.5}$ L/kg at 1 ng/L in the low-TOC soil. The K_D value increased with increasing perfluorocarbon chain length, exceeding PFAS sorption to biochar in the low ng/L concentration range. This result indicates that the mechanism behind the strong PFAS sorption to Fe-char was mainly van der Waals dispersive interactions between the hydrophobic PFAS-chain and the aromatic π-electron systems on nanopore walls within the Fe-char matrix.

Overall, this study indicates that industrial byproducts can provide sustainable and cost-effective materials for soil remediation. However, the sorbent needs to be tailored to the type of soil and type of contamination.

---

* Corresponding author at: Norwegian Geotechnical Institute (NGI), Department of Environmental Engineering, PB 3930 Ullevaal Stadion, Oslo 0806, Norway.
E-mail address: gudny.okkenhaug@ngi.no (G. Okkenhaug).

1. Introduction

In the EU, more than 650,000 contaminated soil sites have been registered in national and regional inventories (JRC, 2018). Defense force activities are an important source of soil contamination, where challenges are provided by metal and metalloid contamination at shooting ranges and *per-* and polyfluorinated alkyl substance (PFAS) contamination from firefighting foams (aqueous film-forming foams, AFFFs) related to firefighting training areas (Okkenhaug et al., 2016, Hale et al., 2017, Mahinroosta and Senevirathna, 2020). Soil remediation involves large mass volumes and high costs, and there is a need to develop sustainable cost-effective remediation strategies.

More than 5000 types of PFASs have been produced and used for various domestic and industrial applications. The most studied PFASs are perfluorooctane sulfonate (PFOS), perfluorooctanoic acid (PFOA), and perfluorohexane sulfonate (PFHxS) because of the ubiquity of these types of PFASs in the environment due to their use in AFFFs (Mahinroosta and Senevirathna, 2020).

Shooting range soils are a significant source of lead (Pb), cupper (Cu) and antimony (Sb) soil contamination (Johnson et al., 2005, Okkenhaug et al., 2018). As shown in previous studies, weathering and corrosion of spent bullets lead to mobilization of metals, and Sb may lead to severe soil and water contamination (Heier et al., 2009, Okkenhaug et al., 2016, Okkenhaug et al., 2018). In shooting range soil and soil water, Pb and Cu are present mainly as freely dissolved cations (Pb^{2+}, Cu^{2+}) or are associated with inorganic or organic ligands related to dissolved organic carbon (DOC). Antimony, on the other hand, mainly occurs as the negatively charged pentavalent species $Sb(OH)_6^-$ (Okkenhaug et al., 2018).

In the remediation literature, the focus has been on the treatment of PFASs in aqueous environments, whereas the treatment of soils has been more scarcely studied (Mahinroosta and Senevirathna, 2020). Because of the physiochemical properties of PFASs such as a high melting point and low vapor pressure, PFAS soil remediation by simple thermal treatments (except high-temperature pyrolysis), air sparging, or soil vapor extractions is not feasible (Kucharzyk et al., 2017). Immobilization methods (chemical stabilization) provide the main remediation alternatives for PFAS-contaminated soil (Mahinroosta and Senevirathna, 2020). In general, carbon-based materials usually show strong affinity toward organic pollutants via various mechanisms, such as H–bonding to functional groups and strong van der Waals dispersive forces between contaminants and aromatic micropore surfaces (Ahmad et al., 2014; Inyang and Dickenson, 2015).

For PFASs, different sorbents have been used in the laboratory as well as in the field, where a high immobilization effect has been achieved with carbonaceous materials such as activated carbon (AC) and biochar, with up to more than 99% reduction in PFOS leaching (Kupryianchyk et al., 2016, Hale et al., 2017, Silvani et al., 2019, Sorengard et al., 2019, Mahinroosta and Senevirathna, 2020, Sormo et al., 2021).

Treatment by carbonaceous materials has also been investigated for the immobilization of metals and Sb (Beesley et al., 2011; Vithanage et al., 2015; Xu et al., 2016). Biochar was shown to have a significant effect on reducing Pb and Sb concentrations in water leachate from shooting range soils in the ranges of 40–61% and 12–90%, respectively (Silvani et al., 2019). The retention effect for metals and Sb in carbonaceous materials is based on electrostatic interactions with polar functional groups on the char surface (Beesley et al., 2011; Ahmad et al., 2014; Du et al., 2014).

Other frequently used sorbents for contaminated shooting ranges are Fe-based materials. Fe oxyhydroxide and zerovalent iron (Fe^0) are among the most studied and commonly used reactive amendments for soil stabilization (O'Day and Vlassopoulos, 2010, Okkenhaug et al., 2013, Okkenhaug et al., 2016). The sorption effect is based on the reaction with surface hydroxyl groups (FeO^-, $FeOH^0$, $FeOH_2^+$), and due to the amphoteric feature with variable surface charge, Fe oxyhydroxides can create surface complexes with both cationic and anionic species, such as Pb^{2+}, Cu^{2+} and $Sb(OH)_6^-$ (Dzombak and Morel, 1990; Filella et al., 2002; Trivedi et al., 2003). Adding Fe oxyhydroxides (e.g., ferrihydrite, goethite, hematite) and Fe^0-grit has been shown to be successful in remediating heavy metals

and antimony in shooting range soil (Okkenhaug et al., 2013, Okkenhaug et al., 2016).

Fe and Al oxyhydroxides may also have an adsorption effect on PFASs in soil. Wei and coworkers found that in addition to hydrophobic interactions, ion exchange, surface complexing and hydrogen bonding might play a role in PFOS sorption onto soil samples, where parameters such as the Al and Fe oxide content increased the sorption strength of PFOS (Wei et al., 2017). Moreover, micropores of minerals and metal oxides are important in PFAS adsorption because they provide additional reactive sites (Du et al., 2017; Kucharzyk et al., 2017; Xiao et al., 2017). In contrast to carbonaceous materials, the hydrophilic heads of PFAS molecules show strong electrostatic interactions with oxyhydroxide surfaces (Wei et al., 2017).

In general, effective sorbents for soil stabilization should have high and irreversible sorption affinity for the target contaminants, as well as high contaminant loading capacity. Most sorbents tested to date have been manufactured for use as sorbents, and both activated biochar and iron oxyhydroxides are rather expensive, reaching 1000 US$ per ton, making it challenging to achieve cost-effective soil stabilization. An innovative, alternative solution may be the utilization of industrial byproducts and wastes. Such materials may represent sustainable, low-cost solutions, reusing resources and supporting the circular economy. Due to the high Fe oxyhydroxide and carbon contents in industrial byproducts, we hypothesized that these materials would provide good sorbents for both PFAS and heavy metal contaminants in soils.

This hypothesis was tested by investigating the effect of two different industrial waste byproducts, i.e., slag and Fe-char, on the leaching of PFASs and of Pb and Sb from contaminated soils from a firefighting area at a military airport and a shooting range, respectively. This study is among the first to study industrial byproducts from titanium and iron processing for utilization as soil sorbents and definitely the first to do so for PFASs and Sb. Moreover, the present study is the first to investigate the effect of soil organic matter by using soils with strongly variable total organic carbon (TOC) contents. Detailed chemical and physical characterizations of the sorbents were carried out to understand the sorption mechanisms.

2. Materials and methods

2.1. Sorbents

The Fe–rich sorbents used in this study are byproducts from the mineral industry, originating from the production of titanium oxide and iron oxide from ilmenite. The nonmagnetic Fe-char, hereafter called only "Fe-char", is a byproduct of prereduction where fossil coal is added as a part of the process (B in Fig. S1 in the Supporting information, SI). A second sample, called "slag", originated from the iron treatment plant (A in Fig. S1). Both slag and Fe-char were dried at 105 °C and sieved (<4 mm) prior to use.

2.2. Soils

Four soils contaminated with either heavy metals (Pb and Sb) or PFASs were collected and distinguished according to their organic carbon content. Low-TOC (1.6% TOC) and high-TOC (34.2% TOC) PFAS soils were provided by the Norwegian Defense Estates Agency from Rygge Military Airport, Norway, an area polluted with firefighting foam containing PFASs (59.3732 N, 10.7935 E). Five subsamples were mixed from the upper organic horizon for the high-TOC sample, while the low-TOC sample was collected from the eluvial and illuvial mineral horizons below in the podzol. Low-TOC (5.2% TOC) and high-TOC (10.2% TOC) shooting range soils were provided by Lindum AS, sampled at the Tittelsnes military shooting range in Norway (59.7231 N, 5.5156 E) on 1 July 2017 in combination with site excavation and remediation (Silvani et al., 2019). Five subsamples were mixed from sandy masses from the backstop berm for the low-TOC soil sample and a peatland adjacent to the backstop berm for the high-TOC soil sample. Soils were dried at room temperature and sieved (<2 mm). PFAS soil samples were analyzed for the total PFAS content in triplicate and screened for aliphates (C5–C35) using GC–MS according to

SPI 2011 and polycyclic aromatic hydrocarbons (PAHs) using GC–MS according to ISO 18287 by Eurofins Norway.

2.3. Batch experiments with soil and sorbents

2.3.1. Shooting range soils

Based on the EN 12457-2 method, which was detailed by Hale et al. (Hale et al., 2017) and Kupryianchyk et al. (Kupryianchyk et al., 2016) with modifications, batch experiments were conducted in triplicate to determine the sorption of Sb and Pb to Fe-rich sorbents (slag or Fe-char) in contaminated shooting range soil. In each polyethylene tube, 4 g of untreated soil (high- and low-TOC) were mixed together with sorbents at 0%, 5%, 10% and 20% dw. Then, 40 mL deionized water (Millipore, >18 MΩ·cm) was added to 50-mL centrifuge tubes (L/S 10 L/kg) and allowed to reach equilibrium at room temperature (20 °C) in a table shaker for 7 days (120 rpm). Earlier work revealed that 7 days was sufficient to reach equilibrium between soil, sorbent and water (Martínez-Lladó et al., 2008). The pH and electrical conductivity (EC) of the slurries were measured immediately after shaking. Thereafter, the liquid and solid phases were separated by centrifugation at 3000 rpm for 20 min. An appropriate aliquot of the supernatant was removed and filtered through a 0.45-μm filter (polyethersulfone, VWR). The filtrate was split into two fractions for (i) elemental (including Sb and Pb) analysis, preserved in 10% double-distilled HNO_3, and (ii) anion and dissolved organic carbon (DOC) analysis, stored at −20 °C.

Triplicate blank samples with sorbents but without soil were treated and analyzed in the same way as the amended batches.

2.3.2. PFAS-contaminated soils

Sorption of PFAS contamination in soils to the sorbents was investigated by batch experiments with soil slurries in 0.5-L polyethylene bottles, according to the EN 12457-2 method, which was detailed by Hale et al. (Hale et al., 2017) and Kupryianchyk et al. (Kupryianchyk et al., 2016), with modifications, and was also analogous to Silvani et al. (2019). First, 40 g dw of PFAS-contaminated soil was mixed with sorbents at different dosages (0%, 1%, 5%, 10% and 20% dw). Then, 400 mL of Milli-Q water (L/S = 10) was added to each bottle, followed by 14 days of shaking (table shaker, 100 rpm) and 2 days of sedimentation. The pH and EC of the solution were measured immediately after shaking. Thereafter, the bottle was centrifuged at 3000 rpm for 20 min and vacuum-filtered through a 1.2-μm glass microfiber filter (Whatman, grade GF/C). An aliquot of each sample (~300 mL) was stored at 4 °C before PFAS and DOC analysis.

2.4. Characterization of sorbents

The Brunauer-Emmett-Teller (BET) specific surface areas (SSAs) and pore size distribution of both sorbents were determined based on both N_2 and CO_2 adsorption–desorption isotherms, performed on a Quantachrome Autosorb I gas adsorption instrument, with N_2 analysis at 77 K and CO_2 analysis at 273 K. N_2 adsorption investigates pores larger than 1.5 nm, while CO_2 adsorption analyzes pore sizes between 0.3 and 1.5 nm in size (Kwon and Pignatello, 2005). Density functional theory (DFT) and BET analysis were used to interpret CO_2 and N_2 adsorption, respectively.

SEM was conducted using a Zeiss EVO 50 EP scanning electron microscope at an accelerating voltage of 20 kV, while EDX was performed by an INCA Energy 350 system with an X-Max^N 80 silicon drift detector installed.

Combustion of 10 mg of finely milled sorbent at 375 °C followed by in situ acidification with 30 μL of 1 M HCl ("CTO-375" method) was employed to measure BC (Gustafsson et al., 2001). This operational method is used to define and isolate BC, and it has become widely accepted and implemented. Dry and finely ground sorbent (10 mg in Ag capsules) was heated at 375 ± 2 °C for 18 h under an air flow. The BC content of the sorbents was measured as the TOC of the combusted residues.

The crystal structures of the sorbents were investigated using XRD with a Bruker D8 Advance diffractometer with Cu Kα radiation (λ = 1.5418 Å) operating at 40 kV and 250 mA.

2.5. Soil and sorbent decomposition

Soil and sorbent samples were decomposed by microwave digestion (Ultraclave Millestone; predigestion up to 100 °C for 30 min and digestion up to 260 °C for 1 h); up to 0.25 g of sample was weighed and added to Teflon tubes, and two different combinations of acids were used because of the effectiveness in attacking the crystal mineral structure and converting different types of compounds into soluble salts. The first combination consisted of ultrapure nitric (10% v/v) and hydrochloric (2% v/v) acids for stabilization of mercury and determination of elements such as Cu, As, Pb, Zn, Ni, Cd and Ca. The second consisted of a combination of nitric (10% v/v) and hydrofluoric (2% v/v) acids for the determination of Sb, V, Na and Ti. After decomposition, the samples were diluted with 18 MΩ water to 50 mL prior to analysis by ICP–MS (see below).

2.6. Chemical analysis

Total elemental analysis from the acid digestion of slag and charcoal was determined by inductively coupled plasma–mass spectrometry (ICP–MS) on an Agilent 8800 QQQ instrument with He and O_2 gas flows to remove some polyatomic interferences. The analyses were conducted with Bi, In, Au and Rh introduced online as internal standards to achieve control over plasma physical interferences during analysis.

Two soil-certified reference materials, NIST 2709a and NIST 2710a, were used to determine the recoveries obtained by decomposition procedures. Recoveries for the most important metals, Pb and Sb, were 98% and 94%, respectively.

Aqueous concentrations of Sb and Pb, as well as the main cationic metals (Na, Mg, Al, K, Ca, Fe, Ti, V, Cr, Ni, Zn, Cu), in the batch tests were also analyzed using ICP–MS following the procedure described above. Limit of quantification (LOQ) for the elements are given in Table S1 in the SI. The results for Ti, V, Cr, Ni, Zn and Cu are shown in Fig. S2. NIST SRM 1643 e (trace elements in water) was used as the reference material. All analyzed elements were within certified values. The analysis of PFAS concentrations in both soils and leachates was carried out following method DIN 38407-F42 with quantification using LC/MS-MS; details can be found in Hale et al. (2017). The compounds included in the analysis were PFOS, PFOA, PFHxS, PFHxA, PFHpS, PFDS, PFBS, PFBA, PFPeA, PFHpA, PFNA, PFDeA, PFDoA, PFTrA, PFTA, PFHxDA, PFOSA, 4:2FTS, 6:2FTS (H4PFOS), 8:2FTS, HPFHpA, and PF-3,7-DMOA (for details, see Table S4 in the SI). The total PFAS concentration was determined as the sum of the selected compounds.

We designed batch leaching experiments and PFAS analysis experiments in triplicate. PFAS analysis was performed in an accredited laboratory. Prior to PFAS analysis, we added 13 internal isotopically labeled standards to all soil and leachate samples. PFAS identification was based on molecular or fragment ions and retention times, and quantification was performed by comparison with internal isotopically labeled standards. The detection limits for PFASs in soil were 1 mg/kg and were 5 ng/L for PFASs in leachate (Hale et al., 2017). In addition, Kupryianchy et al. demonstrated that PFASs are barely adsorbed by the 2-liter polyethylene bottle and the 0.7-mm polyethersulfone membrane used in the tests (Kupryianchyk et al., 2016).

The dissolved organic carbon (DOC) of all leachates was analyzed by elemental analysis after high-temperature combustion (1030 °C) in a total organic carbon analyzer (TOC–V CPN, Shimadzu Corporation, Japan). Extractable anions (F^-, Cl^-, NO_3^-, SO_4^{2-}) were detected using ion chromatography (IC 5000 Ion Chromatography, Lachat Zellweger Analytics) with a Donax IonPac AS22-Fast column and 0.045 M $NaCO_3$ and 0.14 M $NaHCO_3$ as the mobile phase. pH in water extractions was measured by a pH meter (PHM 210, Radiometer).

Total organic carbon (TOC) in soil samples was analyzed by a Leco Carbon analyzer EC12 60 (St. Joseph, Michigan, USA).

2.7. Data processing

Statistical data treatment was performed using OriginPro 9.1 software. Chemical speciation of Pb and Sb in the leachate from the batch tests was

modeled with the chemical equilibrium model Visual MINTEQ (version 3.1). The thermos.vdb database provided with the software was used for the calculations. For complexation with DOC, the NICA-Donnan model included in Visual MINTEQ was used with parameters for fulvic acid (Milne et al., 2003).

Statistical differences among parameters were calculated using one–way ANOVA followed by the comparison of means based on Tukey's *t-test*. All data shown are the means of triplicates.

The partitioning coefficient (K_D) for PFASs between soil (C_{soil}) and water (C_w) in the unamended soil samples was calculated assuming a linear sorption model (Eq. (1)) and by calculating C_{soil} at equilibrium from the initial soil concentration ($C_{soil,i}$) and the leachable concentration ($C_{leachable}$), which is calculated from Eq. (2) (Eq. (3)):

$$K_D \ (L/kg) = C_{soil} \ (\mu g/kg) \times C_w (\mu g/L) \tag{1}$$

$$C_{leachable} \ (\mu g/kg) = C_w (\mu g/L) \times V_w(L)/M_{soil,dw}(kg) \tag{2}$$

$$K_D \ (L/kg) = (C_{soil,i} \ (\mu g/kg) - C_{leachable} \ (\mu g/kg))/C_w \ (\mu g/L) \tag{3}$$

Hysteresis, i.e., Kd,desorption exceeding Kd,adsorption, can occur if the system experiences kinetic limitations. Therefore, a relatively long equilibration time of 14 d was used for PFASs, whereas previous work on the same systems show that 14–28 d was sufficient for PAHs that are more strongly sorbing and more hydrophobic (Cornelissen et al., 2006).

Standard deviations in K_D were calculated, including propagation of random errors (see, e.g., (Miller and Miller, n.d.)).

OC-normalized sorption coefficients for the soils were calculated by the following equation (Eq. (4)):

$$K_{OC} \ (L/kg) = K_D \ (L/kg)/f_{OC} \tag{4}$$

Where f_{OC} is the OC fraction of the soil.

Sorbent-water partitioning is best described by a nonlinear sorption model such as the Freundlich isotherm (Cornelissen et al., 2005) (Eq. (5)):

$$C_{sorbent}(\mu g/kg) = K_{F,sorbent}(L/kg) \times C_w^{nF,sorbent} \ (\mu g/L) \tag{5}$$

where $K_{F,sorbent}$ and $n_{F,sorbent}$ are the Freundlich coefficient and exponent, respectively. Freundlich coefficients are a measure of sorption strength, which is mainly determined by sorption affinity, theoretically to a distribution of various site sorption energies (Schwarzenbach et al., 2016). Freundlich exponents are a measure of sorption linearity, which is determined by the capacity of the sorbent for the sorbate studied; a lower n-value results in lower sorption at higher concentrations due to saturation of the limited number of sorption sites. A mass balance for a given PFAS compound (m_{tot}) in an amended sample includes the mass of PFAS in solution (m_w), soil (m_{soil}) and sorbent ($m_{biochar}$) at equilibrium (Eq. (6)):

$$
\begin{aligned}
m_{tot} \ (\mu g) &= m_w(\mu g) + m_{soil}(\mu g) + m_{biochar}(\mu g) \\
&= C_w \left(\frac{\mu g}{L}\right) \times V_w(L) + C_{soil}\left(\frac{\mu g}{kg}\right) \times M_{soil}(kg) + C_{biochar}\left(\frac{\mu g}{kg}\right) \\
&\quad \times M_{biochar}(kg)
\end{aligned}
\tag{6}
$$

m_{tot} at equilibrium is equal to the initial soil concentration $C_{soil,i}$ before leaching. Combining the linear sorption model for the unamended soil (Eq. (3)) with the Freundlich isotherm (Eq. (5)) in the total mass balance

of the amended system at equilibrium (Eq. (6)) then yields the following expression (Eq. (7)):

$$
\begin{aligned}
m_{tot}(\mu g) &= C_w(\mu g/L) \times V_w(L) + K_D(L/kg) \times C_w(\mu g/L) \times M_{soil}(kg) \\
&\quad + K_{F,sorbent}((\mu g/kg)/(\mu g/L)n) \times C_w^{nF,sorbent}(\mu g/L) \times M_{sorbent}(kg)
\end{aligned}
\tag{7}
$$

Here, $K_{F,sorbent}$ and $n_{F,sorbent}$ were calculated for a range of sorbent doses ($M_{sorbent}$), and the resulting C_W was calculated by rearranging Eq. (6), plotting $Log(m_{tot} - C_WV_W - K_DC_WM_{soil})$ vs. $LogC_W$. In this way, a linear regression was conducted with $n_{F,sorbent}$ as the slope and $K_{F,sorbent}$ as the intercept. $K_{F,sorbent}$ values were calculated both on 1 ng/L and 1 μg/L normalization for PFBS, PFBA, PFPeA, PFHxA, PFHxS, PFHpA, PFHpS, PFOA and PFOS. Standard deviations were reported in the linear regression parameters.

3. Results and discussion

3.1. Soil and sorbent characteristics

Selected physicochemical properties of contaminated shooting range soils are given in Table S2. Both soils were neutral to moderately alkaline (pH 7.40 and 8.19 for organic and mineral soil, respectively; Table S2), and the TOC content of high-TOC metal-contaminated soil (10.2%) was twice that of low-TOC soil (5.2%). Pb contamination is dominant in both soil types (4300 mg/kg for high-TOC soil, 6600 mg/kg for low-TOC soil), and they can be classified as hazardous waste according to Norwegian waste legislation (Norwegian Ministry of Climate and Environment, 2004). The Sb content was 100 mg/kg for high-TOC soil and 210 mg/kg for low-TOC soil.

Selected physicochemical properties of PFAS-contaminated soils are given in Tables S2-S4. The majority of the PFAS content in soil consisted of PFOS, at 83% and 89% in high- and low-TOC soils, respectively, followed by PFHxS, at 9.2% and 5.3%. PAHs were detected in the low-TOC soil (ΣPAH16 0.33 ± 0.16 mg/kg, Table S5), but no aliphates were present. No PAHs (<0.045 mg/kg, Table S5) but long-chain aliphates (C16–C35, 513 ± 6 mg/kg) were detected in the high-TOC soil. It is uncertain whether these aliphates stem from the use of fuel at firefighting training facilities or from the natural organic matter of the O-horizon.

The selected physical–chemical properties of the sorbents are shown in Table 1, including the main metal contents.

Both sorbents showed high Fe contents of 400 g/kg (slag) and 180 g/kg (Fe-char), reflecting the industrial processes from which they originated (Table 1). Other elements with elevated concentrations in both sorbents were aluminum (Al) and Ti, in addition to calcium (Ca), which had concentrations of 67 g/kg (slag) and 22 g/kg (Fe-char). Calcium in the slag originates from the addition of lime to improve slag formation, whereas the Ca and K sources in Fe-char could be related to the addition of bentonite in the pelletizing plant for illite. Fe-char showed a high concentration of total carbon (TC, 27.8%), originating from fossil coal added during the prereduction process. The carbon content of the slag was lower (8.32%), although with the same origin as in Fe-char (added fossil coal). The BC content in the Fe-char (6.55%) was higher than that in the slag (0.81%), suggesting that there was more condensed, hard C in the Fe-char than in the slag.

The initial concentrations of Pb and Sb in the sorbents were low in both slag (14 mg/kg Sb, 3.2 mg/kg Pb) and Fe-char (0.32 mg/kg Sb, 11 mg/kg Pb) (Table 1).

XRD analysis confirmed that both sorbents contained a high Fe content (Table S6). For the slag, Fe-minerals were mainly observed, namely, iron

Table 1

pH, total carbon (TC) and total content of selected elements (ICP–MS) of the sorbents used in the study.

	pH	TC	BC	Fe	Mg	Al	K	Ca	Ti	V	Cr	Ni	Cu	Zn	Sb	Pb
		%	%	g/kg	g/kg	g/kg	g/kg	g/kg	g/kg	g/kg	g/kg	g/kg	mg/kg	mg/kg	mg/kg	mg/kg
Slag	11.62	8.32	0.81	400	2.8	5.3	<0.17	67	3.2	0.26	0.18	0.21	93	17	14	3.2
Fe-char	4.66	27.8	6.55	180	7.4	9	24	22	1.4	0.03	0.03	0.042	32	250	0.32	11

(Fe), wuestite (FeO), siderite (FeCO$_3$) and hematite (Fe$_2$O$_3$), whereas Fe-char contained magnetite (Fe(II); Fe(*III*)O$_3$), quartz (SiO$_2$) and clay minerals, with the last components indicating bentonite residues.

Leaching with water revealed a high pH of the slag (pH 11.62), reflecting the high content of carbonates and hydroxides in the material. The pH of the Fe-char was substantially lower (pH 4.66). The water leachable fraction of main cations and anions was low for both sorbents (Table S7).

SEM images (Fig. 1) and EDX mapping analysis are shown in Figs. S3 and S4. As shown in Fig. 1A and B, the morphology of the slag showed significant clusters of pure iron and other Fe-based minerals. Compared with that of the slag, the morphology of Fe-char appeared to be smoother, with some obvious layered structures (Fig. 1C and D). These layered structures are mainly compounds occurring in lignite originating from coal mining, such as quartz and graphite (Sarlaki et al., 2021). Most of the layers showed broken edges, which might be due to the high cooling rate during quenching of the charcoal in the smelting and granulation process. Noticeably, nodules of varying sizes were observed on the surfaces of both sorbents, partially or wholly within the sorbent matrix. These nodular particles are suggested to be Fe–oxides, especially Fe$_2$O$_3$ and Fe$_3$O$_4$ (Zhang et al., 2013), which is in good agreement with the XRD results.

The N$_2$-BET SSAs (pores >1.5 nm) of slag and Fe-char were 6.8 and 64.5 m^2/g, respectively (Table 2). At 6.8 m^2/g, the surface area of the slag was low, with a pore volume of 0.012 mL/g, indicating that the Fe–rich slag material contained few micro- and nanopore structures. Fe-char, although exhibiting higher surface areas than slag, showed a substantially lower pore volume (0.026 mL/g) and surface area than the most carbonaceous geosorbent ("black carbon") materials, such as biochar and activated carbon, which can have surface areas over 1000 m^2/g (Cornelissen et al., 2005; Ghosh et al., 2011; Sørmo et al., 2020). The CO$_2$-based surface area and pore volume (nanopores between 0.3 and 1.5 nm in size) were substantially higher than the N$_2$-based surface area and pore volume. The CO$_2$ surface area for Fe-char was 214.5 m^2/g. However, the nanopore surface areas

Table 2
Surface area and total pore volume of slag and Fe-char based on N$_2$ adsorption (pores >1.5 nm) and CO$_2$ adsorption (pores 0.3–1.5 nm).

Sorbents	BET surface area > 1.5 nm N$_2$ (m^2/g)	Total > 1.5 nm pore volume; N$_2$ (cm^3/g)	DFT surface area 0.3–1.5 nm; CO$_2$ (m^2/g)	Total pore volume 0.3–1.5 nm; CO$_2$ (cm^3/g)
Slag	6.8	0.012	13.3	0.005
Fe-char	64.5	0.026	214.5	0.057

were also smaller than those reported earlier for biomass-based and fossil-based activated carbon (Amstaetter et al., 2012) and biochar (700–900 m^2/g) (Cornelissen et al., 2013). Nanopore surfaces may endow Fe-char with a high affinity for both heavy metals and organic pollutants via strong interactions with functional groups and aromatic moieties, respectively, at the walls of the extensive pore system (Amstaetter et al., 2012; Ahmad et al., 2014). From the CC and CF bond lengths, the molecular sizes of many types of PFASs are on the order of 0.3 × 0.3 × 1.5–2 nm. This estimate is confirmed by the molar volume of approximately 180–300 cm^3/mol, i.e., approximately 0.2–0.5 nm^3 per molecule, for PFASs with 6–8 C units (Kim et al., 2015), and thus, they will just fit inside the 0.3–1.5 nm pores probed by CO$_2$ adsorption isotherms. The porosity of Fe-char (<6%) was lower than that of other widely used carbon materials because this material was only partly carbonaceous (28% C).

3.2. Effect of sorbents on the immobilization of Pb and Sb in shooting range soils

3.2.1. Untreated shooting range soils

The water-extractable concentrations of Pb and Sb in untreated high-TOC shooting range soil were 303 and 180 µg/L, respectively; for low-TOC soil, these values were 243 and 307 µg/L (Table S7). For both soils, the amount of Sb leaching exceeded the leaching limits for ordinary waste landfills (70 µg/L or 0.7 mg/kg, batch shaking test) in EU landfill
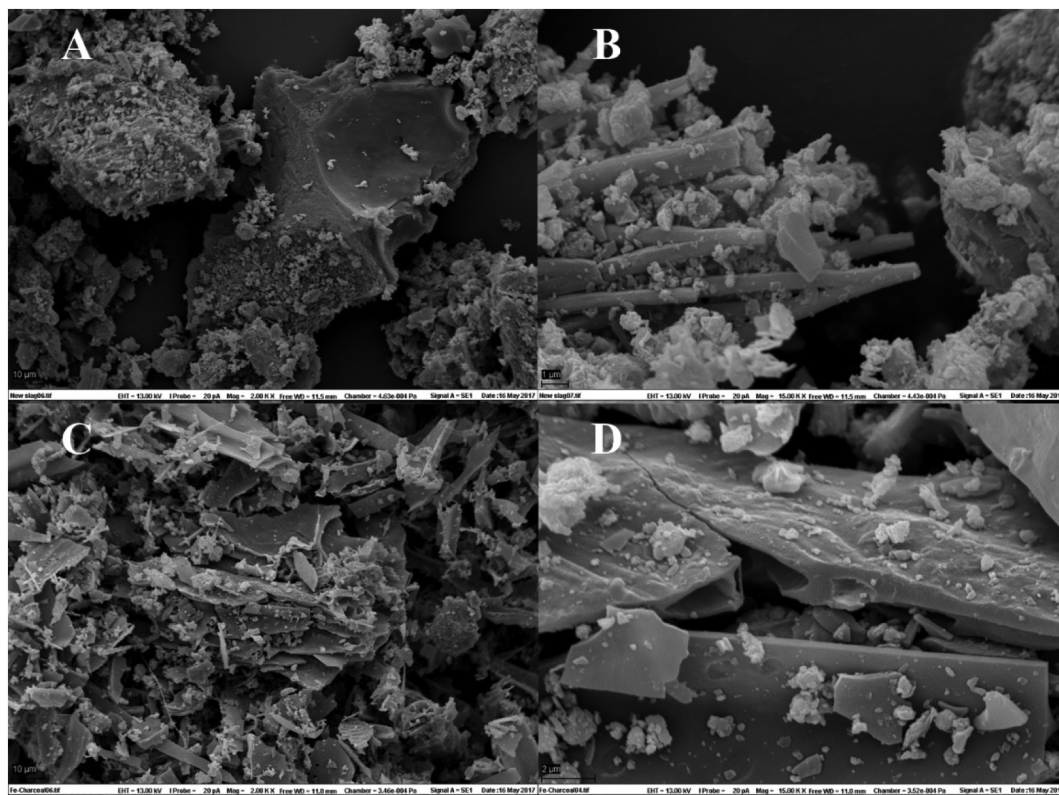

Fig. 1. SEM images of adsorbents: (A) Slag (magnification of 2.00 K); (B) Slag (magnification of 15.00 K); (C) Fe-char (magnification of 2.00 K); (D) Fe-char (magnification of 15.00 K).

legislation (European Union, 1999), whereas that of Pb leaching was within the criteria for ordinary landfills (1000 μg/L or 10 mg/kg, batch shaking test). Comparing the distribution coefficient (K_D) for Pb in high-TOC ($K_D = 10^{4.43}$ L/kg) and low-TOC ($K_D = 10^{4.15}$ L/kg) soils with that for Sb in high-TOC ($K_D = 10^{2.84}$ L/kg) and low-TOC ($K_D = 10^{2.74}$ L/kg) soils showed that Sb was substantially more extractable than Pb. Geochemical modeling of the leachate water (input data given in Table S8) indicated that Pb was mainly associated with DOC, whereas Sb largely occurred as a freely dissolved oxyanion ($Sb(OH)_6^-$).

3.2.2. Effect of sorbents on the immobilization of Pb and Sb in shooting range soils

Adding slag to shooting range soils significantly decreased the Sb concentration in soil water ($p < 0.05$) for both high- and low-TOC soils at 10 and 20% amendment, with the best performance observed in the high-TOC soil (90% reduction in leaching at 10% slag amendment) (Fig. 2 A1). Unfortunately, no sorption isotherms could be constructed for Pb and Sb, as the effectiveness of the sorbents varied too much with dosage. The results are in accordance with findings in the literature, where Sb was effectively immobilized using various Fe-based sorbents, e.g., iron grit and ferric oxyhydroxide powder, with a reduction in leaching of 89–90% for Sb and 89–99% for Pb (Okkenhaug et al., 2016). The stronger Sb sorption effect in the high-TOC shooting range soil could be explained by the lower pH (pH 7.64–7.71, Fig. 3) than that in the low-TOC soil (pH 7.90–8.19), leading to more positively charged sites on metal oxides in the slag. The sorption edge of Sb on Fe oxyhydroxides depends strongly on the material, where small changes in pH result in substantial changes in the Sb sorption capacity (Leuz et al., 2006). The simultaneously increased DOC concentration (Fig. 3)

does not outweigh the positive immobilization effect. Negatively charged organic acids compete for the same mineral oxide sites as $Sb(OH)_6^-$. Similar to that of the untreated soil, geochemical modeling of the 10% slag-amended soil indicated that Sb is present as a negatively charged oxyanion. Furthermore, Ca can play an important role in the sorption of Sb due to the formation of Ca antimonate precipitates (Okkenhaug et al., 2011). However, the Ca concentrations in the slag (67 g/kg, Table 1) and slag-amended soil eluates (44–102 mg/L) are not high enough to exceed the saturation of Ca antimonates, indicating that the decrease in Sb content is based on sorption (Table S9).

Adding slag to high-TOC soil also decreased the Pb concentration in soil water by 54% (20% slag); however, it was not as effective as Sb. Contrary to expectations, the 5 and 10% slag amendments to the low-TOC soil resulted in significant increases in Pb leaching (Fig. 2, A2). The low Pb total concentration and leaching (3.2 mg/kg, Table 1; 0.22 μg/L) from the pure slag exclude any contamination from the sorbent itself. Relatively stable pH and DOC concentrations (Fig. 3B) do not explain this increased Pb mobility under 5% and 10% slag amendments. Geochemical modeling of the water extracts showed undersaturation of Pb (cerussite, hydrocerussite) and Sb (Ca antimonate) minerals (Table S9), indicating that Pb and Sb mobility and leaching are governed by sorption, not precipitation.

The addition of Fe-char to the contaminated shooting range soils gave a moderate reduction in Sb leaching from both high-TOC and low-TOC soils, showing reductions of 71% and 22%, respectively, with 10% amendment (Fig. 2 B1 and B2). This sorption effect is most likely explained by the Fe oxyhydroxides in the material. The lower reduction in Sb leaching observed for Fe-char (~20% and 70% of low- and high-TOC soils, respectively, with 10% amendment) than for the slag (~60% and 90% of low- and high-TOC
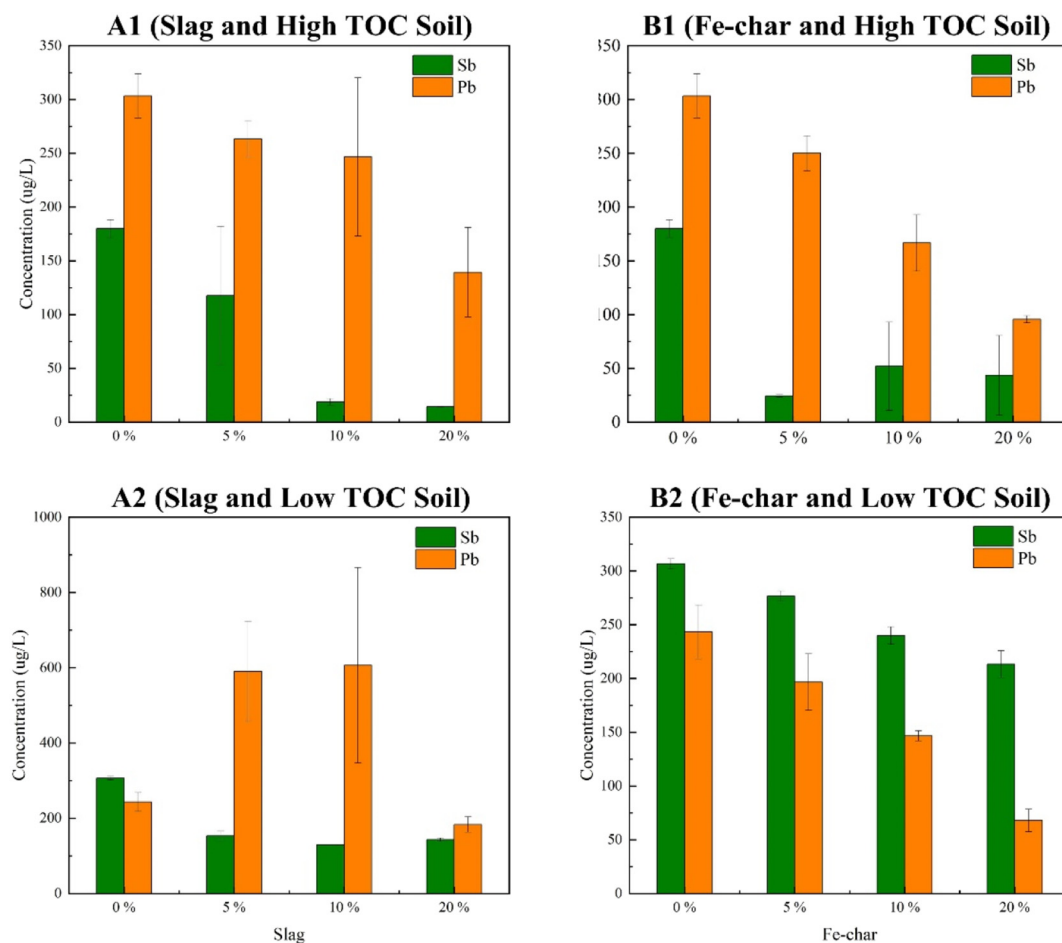

Fig. 2. Variation in water-extractable Pb and Sb concentrations in high-TOC (A1 and B1) and low-TOC (A2 and B2) shooting range soils with the addition of slag (A1 and A2) or Fe-char (B1 and B2) at dosages of 0, 5, 10 and 20%.
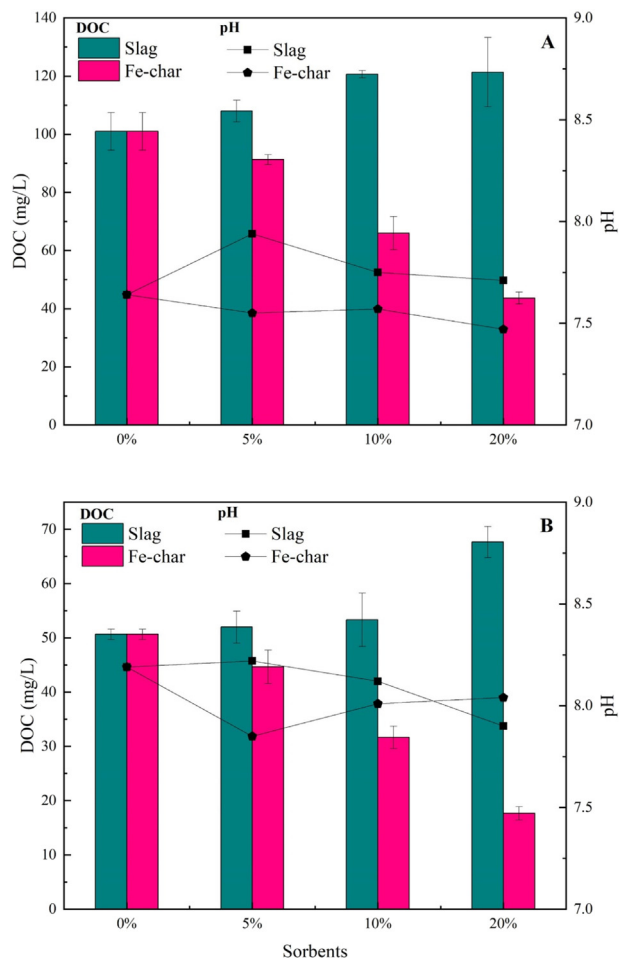
Fig. 3. Variation in DOC and pH in the leachate of high-TOC (A) and low-TOC (B) shooting range soils as a result of the addition of different sorbents.

Fe-char. No oversaturation of Pb minerals (e.g., cerussite, hydrocerussite, $Pb(OH)_2$) was observed in the geochemical modeling of the water extracts of high-TOC soil and Fe-char (Table S9).

Sb and Pb in both soils were simultaneously immobilized by Fe-char amendment; however, leaching of Sb at 213 μg/L, which equals 2.13 mg/kg, still exceeded the criteria for Sb leachate from ordinary waste land-fills (0.7 mg/kg).

3.3. Effect of sorbents on the immobilization of PFASs in soils

For the leaching data of PFAS-contaminated soils, the results in the main paper are focused on the PFOS, PFHxS and sum PFAS (the sum of all detected PFASs) concentrations. The sorption isotherm parameters, however, are shown for all nine PFAS compounds (PFBS, PFHxS, PFHpS, PFOS, PFBA, PFPeA, PFHxA, PFHpA and PFOA), for which a sorption iso-therm could be obtained (Table 3).

The high-TOC soil (TOC 34.2%) was significantly more acidic (pH 4.9) than the low-TOC soil (TOC 1.61%; pH 7.8). Low-TOC soil exhibited a total PFAS content of 3800 ± 240 μg/kg, approximately 3 times higher than that of the high-TOC soil (1200 ± 80 μg/kg). In total, 18 different PFAS compounds were detected above the detection limit (0.2–0.3 μg/kg).

Sorption of PFASs to the unamended low-TOC soil was weak, with K_D values between $10^{-0.34}$ and $10^{1.14}$ L/kg (Table 3). The high-TOC soil showed stronger sorption, with K_D values between $10^{1.45}$ and $10^{2.93}$ L/kg. Sorption to the soil was stronger for sulfonate compounds (PFSAs) than for perfluorinated acids (PFCAs), and the sorption strength increased with perfluorocarbon chain length within each compound class. The OC-normalized K_{OC} values were similar for both soils and in accordance with literature values (Fabregat-Palau et al., 2021) (Table 3). The values for $K_{D,soil}$, however, deviated slightly from those obtained by Silvani et al. (2019). We think there could be three main reasons: 1) soil heterogeneity, 2) differences in soil pretreatment, and 3) aging of the soil, affecting both soil OM and PFAS distribution. However, the main finding that the Fe-char sorbed much more strongly than the soil itself is not influenced by rel-atively minor differences in Kd,soil between the Silvani work and the pres-ent study.

The addition of Fe-char effectively reduced the leaching of all measured PFAS compounds from the low-TOC soil (Fig. 4-Panel B2). For example, the addition of 1 and 10% Fe-char was sufficient to reduce the leaching of the total (sum) detected PFASs by 74 and 99.7%, respectively. Earlier work on sorbent amendment to the same low-TOC PFAS-contaminated soil re-vealed reductions in PFAS leaching of 86% and >99.9% for biochar and ac-tivated biochar, respectively (Silvani et al., 2019). For aqueous film forming foam (AFFF)-contaminated soil with a low TOC between 0.17 and 1.2%,

soils, respectively, with 10% amendment) was probably explained by the lower Fe oxyhydroxide content in the Fe-char (Table 1).

The effect of Fe-char amendment on Pb was substantially stronger than that on Sb, with decreases in leaching of 45% (high-TOC soil) and 40% (low-TOC soil) with 10% amendment. Geochemical modeling indicated that Pb was mainly associated with DOC in the soil water; thus, the reduc-tion in Pb was also most likely coupled with DOC sorption to the char in the

Table 3
Soil-water distribution ratios K_D and K_{OC} for both PFAS soils without sorbent amendment, as well as Freundlich model parameters for the sorption of PFASs to the Fe–based charcoal sorbent (Fe-char) in the presence of low-TOC soil. For the slag sorbent in the low-TOC soil, as well as for both sorbents in the high-TOC soil, no Freundlich regression parameters could be obtained due to weak sorption. Sorption isotherms were derived from regressions based on five points (aqueous concentrations at the various sorbent dosages) unless otherwise noted.

	Number of CF_2 units	Log $K_{D,soil}$ L/kg	Log $K_{OC,soil}$ L/kg	Log $K_{D,soil}$ L/kg	Log $K_{OC,soil}$ L/kg	Log$K_{F,sorbent}$ (ng/kg) / (ng/L)^n = log $K_{D,sorbent}$ at 1 ng/L	Log$K_{F,sorbent}$ (μg/kg) / (μg/L)^n = log $K_{D,sorbent}$ at 1 μg/L	$n_{F,sorbent}$	R^2
		Low-TOC soil		High-TOC soil		Fe-char sorbent in low-TOC soil			
PFBS	4	0.21 ± 0.01	2.00 ± 0.01	1.27 ± 0.01	1.74 ± 0.01	5.11 ± 0.02	3.0 ± 0.1	0.29 ± 0.01	0.996
PFHxS	6	n.d.[c]	n.d.[c]	1.58 ± 0.03	2.05 ± 0.03	5.6 ± 0.1	3.8 ± 0.1	0.40 ± 0.05	0.94
PFHpS	7	0.25 ± 0.02	2.04 ± 0.02	2.11 ± 0.03	2.58 ± 0.03	5.0 ± 0.3[a]	3.7 ± 0.3	0.56 ± 0.15	0.88[a]
PFOS	8	1.14 ± 0.07	2.93 ± 0.07	2.44 ± 0.03	2.91 ± 0.01	6.5 ± 0.2[a]	4.8 ± 0.2	0.43 ± 0.05[a]	0.97[a]
PFBA	3	−0.34 ± 0.01	1.45 ± 0.01	0.49 ± 0.01	0.96 ± 0.01	4.3 ± 0.2	2.0 ± 1.0	0.24 ± 0.10	0.64
PFPeA	4	0.37 ± 0.01	2.16 ± 0.01	0.77 ± 0.01	1.24 ± 0.01	4.63 ± 0.05[a]	2.6 ± 0.1	0.33 ± 0.02	0.990
PFHxA	5	n.d.[c]	n.d.[c]	0.16 ± 0.02	0.63 ± 0.02	5.2 ± 0.2	2.9 ± 0.2	0.26 ± 0.07	0.82
PFHpA	6	n.d.[c]	n.d.[c]	0.55 ± 0.02	1.02 ± 0.02	4.6 ± 0.1[b]	2.6 ± 0.1	0.33 ± 0.05	0.97[b]
PFOA	7	−0.09 ± 0.03	1.70 ± 0.01	1.26 ± 0.02	1.73 ± 0.01	5.2 ± 0.1[b]	3.3 ± 0.5	0.35 ± 0.05	0.98[b]

[a] Regression based on 4 points (below detection for the 20% sorbent dosage).
[b] Regression based on 3 points (below detection for the 10% and 20% sorbent dosages).
[c] n.d., not determined because sorption was so weak that the amount leached into the water exceeded the original amount in the soil.
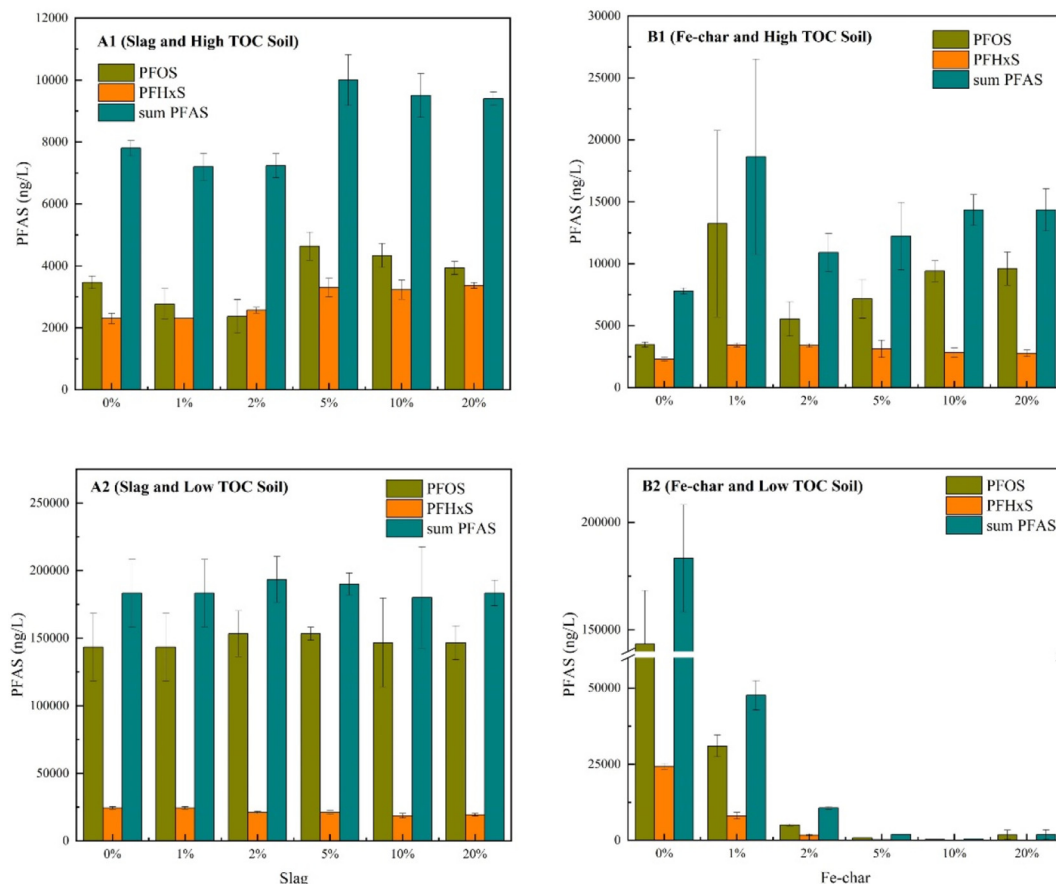
Fig. 4. Effect of sorbent amendment on the leached concentration of PFOS, PFHxS, and sum PFASs (sum of all detected PFASs): A1 and B1) low-TOC soil; A2 and B2) high-TOC soil with the addition of slag (A1 and A2) or Fe-char (B1 and B2).

amendment with commercial activated carbon resulted in a 94% to 99% reduction in leaching (Hale et al., 2017).

Although relatively excellent remediation of PFAS-contaminated soils can be obtained with commercially available activated carbon or modified activated carbon at the same amount used, equally satisfactory results can be obtained by increasing the amount of Fe-char added. In this way, Fe-char was utilized resourcefully. More importantly, Fe-char as an industrial waste byproduct is less expensive than commercial activated carbon, and replacing or partially replacing commercial activated carbon with Fe-char can reduce the cost of remediation of PFAS-contaminated soil (Fig. 4).

The addition of Fe-char to the high-TOC soil did not result in any significant reduction in PFAS leaching (Fig. 4 B2). Thus, Fe-char performed significantly poorer as a sorbent in the high-TOC soil than in the low-TOC soil. The difference in sorbent effectiveness between high- and low-TOC soils can be explained by the high concentrations of organic matter in the high-TOC soil, attenuating the effect of the Fe-char sorbent by pore clogging and competitive sorption to pore walls (Kwon and Pignatello, 2005; Cornelissen and Gustafsson, 2006). This effect of weaker sorption in the presence of high amounts of organic matter has been shown for many hydrophobic compounds, such as PAHs and DDT (Cornelissen et al., 2006, Hale et al., 2009). However, this effect has also been demonstrated specifically for PFASs in AC (Du et al., 2014) and biochar (Sormo et al., 2021). In addition, the high-TOC soil itself sorbed PFASs approximately 30 times more strongly (log $K_D = 10^{2.44}$ L/kg) than the low-TOC soil (log $K_D = 10^{1.14}$ L/kg; Table 3), necessitating stronger sorbents to overcome the sorption of the soil itself and achieve a certain reduction in leaching.

For the addition of slag to either low-TOC or high-TOC soil, no significant ($p < 0.05$) effect on the PFAS leaching concentration was observed (Fig. 4 B1). Slag showed a substantially lower BC content (0.81% BC)

than Fe-char (6.55% BC). Thus, a higher BC content resulted in stronger PFAS sorption, in accordance with the addition of carbonaceous sorbents to soils, resulting in far stronger PFAS binding and much lower leaching (Kupryianchyk et al., 2016, Hale et al., 2017, Sormo et al., 2021). The higher Fe(hydr)oxide content in slag did not appear to exert any effect on PFAS retention in the low-TOC soil at neutral, slightly alkaline pH values (7.48–7.72, Fig. 5).

In the present study, only sorption on amended soil systems was measured. Analyzing sorption isotherms on clean sorbents without soils would have allowed quantification of the soil effect on Kd, giving insight into sorption mechanisms. However, sorbent amendment to field-contaminated soils (not spiked systems) automatically includes the study of the effects of aging, the soil matrix (resulting in pore clogging) and the presence of other chemicals (resulting in competitive effects for limited sorption sites). This fact increases the applicability of the study to the real world.

3.3.1. PFAS sorption parameters for sorbents

Reliable log K_F values were obtained from the sorption isotherms for the Fe-char amended to low-TOC soil, with R^2 values above 0.9 for most compounds. A possible limitation is that the sorption isotherms were based on only 5 points due to the challenge of determining sorption isotherms for environmentally contaminated (i.e., not spiked) soils. However, the isotherm parameters were significant, with R^2 values above 0.9 for 6 out of 9 compounds (Table 3). For the slag sorbent in the low-TOC soil, as well as for both sorbents in the high-TOC soil, no Freundlich regression parameters could be obtained due to weak sorption compared to sorption to the soil itself.

For Fe-char amended to the low-TOC soil, $K_{F,sorbent}$ in units of (ng/kg) / $(ng/L)^n$, i.e., $K_{D,sorbent}$ at 1 ng/L, was observed to vary between $10^{4.3}$ and $10^{6.5}$, again around one order of magnitude lower for PFCAs than for
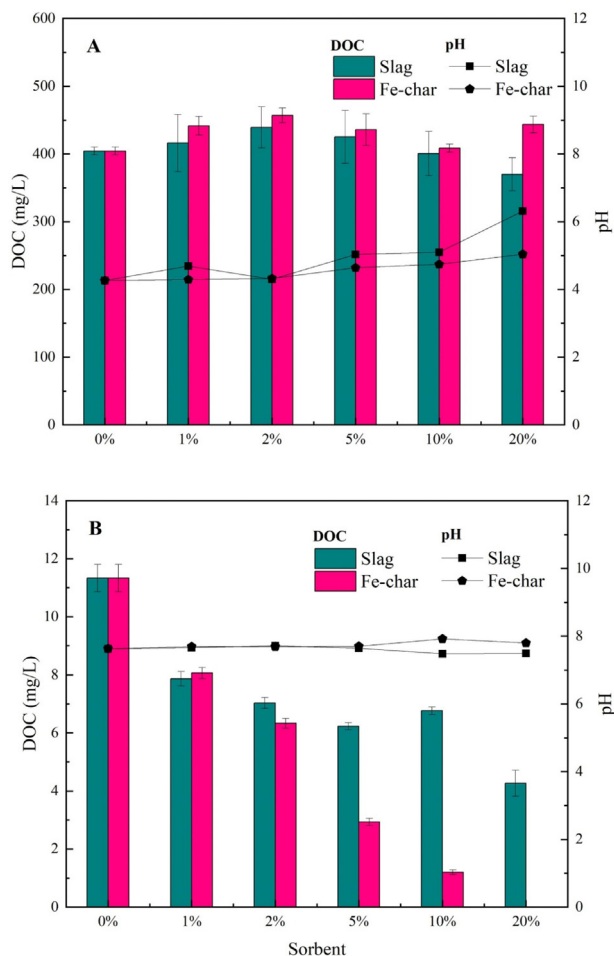
Fig. 5. Variation in DOC and pH in the leachate of high-TOC (A) and low-TOC (B) PFAS-contaminated soils with the addition of different sorbents.

PFSAs, and increasing with perfluorocarbon chain length. The Fe-char used in our study contained a high carbon content (27.8% TC; Table 1), of which almost a quarter (6.55% of total mass; Table 1) was highly condensed, stable black carbon (BC), originating from hard coal, resistant to oxidation at 375 °C. The high BC content of Fe-char can likely explain a large part of its strong sorption of PFASs because the main adsorption mechanism for organic pollutants by carbonaceous materials such as coal, biochar and activated carbon is strong dispersive forces between the hydrophobic parts of the contaminants (in this case, the long perfluorocarbon chains) and the π-electron systems in the aromatic micropore surfaces (Cornelissen et al., 2005; Deng et al., 2012; Ahmad et al., 2014; Inyang and Dickenson, 2015; Wang et al., 2018; Sormo et al., 2021). Increasing sorption strength with increasing perfluorocarbon chain length confirms that the main sorption mechanism for PFASs on Fe-char is likely van der Waals dispersive interactions between the chains and the aromatic pore surface (Du et al., 2014; Sorengard et al., 2019).

Earlier studies have also shown that PFASs may have an affinity for Fe oxides depending on pH, probably due to electrostatic electron donor/acceptor (EDA) interactions between the hydrophilic PFAS head (sulfonate or organic acid) and the polar Fe oxide surfaces (Silvani et al., 2019; Fabregat-Palau et al., 2021). Lu et al. (2016) (Lu et al., 2016) observed the strongest sorption of PFOS to hematite (Fe_2O_3) nanoparticles at pH values below the point of zero charge (PZC), i.e., pH 7.6, at which time hematite has a positive surface charge. The PFSAs investigated in the present work are all strong acids, while the PFCAs are weak acids with low pKa values (<3.8) (Ding and Peijnenburg, 2013), which means that they would all be negatively charged in the soil-Fe-char systems investigated. Furthermore, the PZCs for magnetite and hematite minerals are 6.5 and

5–9, respectively (Schwartz and Zhang, 2003). Thus, it is likely that electrostatic interactions between the negatively charged PFAS functional heads and the positively charged magnetite (33%) and hematite (7%)-rich Fe-char play an important role in the sorption strength of this material. Further indicative of the importance of this mechanism is the fact that the internal surface area of Fe char is small compared to that of ACs and biochars with reported KF values on the same order of magnitude (Sorengard et al., 2019; Sormo et al., 2021). AC surfaces are commonly negatively charged, causing negatively charged PFASs to experience electrostatic repulsion that reduces the net sorption strength despite the strong hydrophobic interactions (Du et al., 2014; Sörengård et al., 2020). In contrast, the positively charged minerals in the Fe-char are expected to increase the sorption strength. Thus, we expect hydrophobic (dispersive electron donor/acceptor of dipole-induced dipole) interactions between aromatic sorbent surfaces and hydrophobic sorbate chains (Cornelissen et al., 2005; Ahmad et al., 2014) for Fe char, but not as strong as those for AC and biochar. In summary, we hypothesize that the sorption of PFASs to Fe-char is a combination of dispersive interactions between aromatic surfaces and hydrophobic PFAS tails, with significant contributions of electrostatic interactions between the hydrophilic PFAS heads and Fe oxides and the aromatic pore surfaces. Mechanistic studies and molecular modeling analogous to the work of De Voogt et al. are needed to quantify these various sorptive interactions (de Voogt et al., 2012).

Values for $K_{D,sorbent}$ at 1 ng/L were 4 to 5 orders of magnitude higher than those for $K_{D,soil}$, indicating that the Fe-char sorbed PFASs 10,000 to 100,000 times more strongly than the low-TOC soil. This result explains the strong reduction in leaching already at modest 1% Fe-char amendments to this soil.

The n_F values were low, ranging from 0.24 to 0.56 (Table 3), indicating strongly nonlinear sorption. This finding was also supported by the $K_{D,sorbent}$ at 1 μg/L being much lower (between $10^{2.0}$ and $10^{4.8}$ L/kg) than that at 1 ng/L. Our findings indicate that Fe-char is a sorbent with a high sorption affinity (strong dispersive and some electrostatic interactions between PFAS molecules and the sorbent pore surface) but with a modest capacity (low amount of strongly sorbing pore surfaces). The low capacity is explained by the low porosity (2.6%; Table 2), resulting in modest internal surface areas of 64 m^2/g (Table 2; pores >1.5 nm) and 215 m^2/g (Table 2; pores between 0.3 and 1.5 nm in size), values that are much lower than those previously observed for biochar (over 500 m^2/g (Silvani et al., 2019)) and activated carbon (over 1000 m^2/g (Ghosh et al., 2011)).

At low ng/L concentrations, however, Fe-char proved to be a very strong sorbent compared to earlier studied biochars and activated carbons. Fe-char showed a $K_{D,sorbent}$ value at 1 ng/L as high as $10^{6.5}$ L/kg, exceeding values for PFOS sorption to biochar and activated biochar of $10^{3.38}$ and $10^{5.49}$ L/kg, respectively, amended to the same soil (Silvani et al., 2019), and for PFOS in different biochars at $10^{3.0}$–$10^{4.6}$ amended to another soil (Kupryianchyk et al., 2016). This result indicates that the industrial byproduct Fe-char shows similar or better sorption characteristics for PFASs than biochars and activated carbons for low to moderately contaminated soils with aqueous concentrations in the ng/L range. For more highly contaminated soils (μg/L to mg/L range), the sorption capacity of Fe-char would be too low for it to be an effective sorbent.

4. Conclusions

In summary, our results indicate that both industrial byproducts slag and Fe-char, which until now had limited or no value, can be used as remediation agents for soils containing a wide array of contaminants, from cations (Pb) to anions (Sb) to polar organic substances (PFASs).

The possible application of the sorbents may encompass both in situ stabilization and stabilization prior to final landfill disposal. All soils used in this study were heavily contaminated and classified as hazardous waste with the need for stabilization prior to landfilling. We showed that adding industrial byproducts can aid in achieving stable, nonreactive hazardous waste with leaching properties in accordance with landfill regulations.

Follow-up studies should include the following: i) amendment of mixtures of slag and Fe-char and possibly other waste fractions from the metal industry; ii) modification of sorbent characteristics; iii) consideration of the long-term stability of the amendment; iv) consideration of the stability of the amendments upon changes in conditions, especially pH; and v) in situ applications of the sorbents in landfills.

CRediT authorship contribution statement

Yaxin Zhang: Conceptualization, Formal analysis, Investigation, Writing – Original Draft. **Gerard Cornelissen**: Conceptualization, Formal analysis, Supervision, Writing – original Draft. **Ludovica Silvani:** Investigation, Writing – Review & Editing. **Valentina Zivanovic**: Investigation, Writing – Review & Editing **Andreas Botnen Smebye:** Writing – Review & Editing. **Erlend Sørmo**: Formal analysis, Writing – Review & Editing. **Gorm Thune**: Resources, Funding acquisition. **Gudny Okkenhaug**: Conceptualization, Investigation, Supervision, Writing – original draft.

Declaration of competing interest

The authors declare that they have no known competing financial interests or personal relationships that could have appeared to influence the work reported in this paper.

Acknowledgments

Appendix A. Supplementary Information

Supplementary data to this article can be found online at https://doi.org/10.1016/j.scitotenv.2022.153188.

References

Ahmad, M., Rajapaksha, A.U., Lim, J.E., Zhang, M., Bolan, N., Mohan, D., Vithanage, M., Lee, S.S., Ok, Y.S., 2014. Biochar as a sorbent for contaminant management in soil and water: a review. Chemosphere 99, 19–33.

Amstaetter, K., Eek, E., Cornelissen, G., 2012. Sorption of PAHs and PCBs to activated carbon: coal versus biomass-based quality. Chemosphere 87 (5), 573–578.

Beesley, L., Moreno-Jimenez, E., Gomez-Eyles, J.L., Harris, E., Robinson, B., Sizmur, T., 2011. A review of biochar's potential role in the remediation, revegetation and restoration of contaminated soils. Environ. Pollut. 159 (12), 3269–3282.

Cornelissen, G., Gustafsson, O., Bucheli, T.D., Jonker, M.T.O., Koelmans, A.A., Van Noort, P.C.M., 2005. Extensive sorption of organic compounds to black carbon, coal, and kerogen in sediments and soils: mechanisms and consequences for distribution, bioaccumulation, and biodegradation. Environ. Sci. Technol. 39 (18), 6881–6895.

Cornelissen, G., Breedveld, G.D., Kalaitzidis, S., Christanis, K., Kibsgaard, A., Oen, A.M., 2006. Strong sorption of native PAHs to pyrogenic and unburned carbonaceous geosorbents in sediments. Environ. Sci. Technol. 40, 1197–1203.

Cornelissen, G., Gustafsson, Ö., 2006. Effects of added PAHs and precipitated humic acid coatings on phenanthrene sorption to environmental black carbon. Environ. Pollut. 141 (3), 526–531.

Cornelissen, G., Rutherford, D.W., Arp, H.P.H., Dörsch, P., Kelly, C.N., Rostad, C.E., 2013. Sorption of pure N2O to biochars and other organic and inorganic materials under anhydrous conditions. Environ. Sci. Technol. 47 (14), 7704–7712.

de Voogt, P., Zurano, L., Serné, P., Haftka, J.J., 2012. Experimental hydrophobicity parameters of perfluorinated alkylated substances from reversed-phase high-performance liquid chromatography. Environ. Chem. 9 (6), 564–570.

Deng, S., Zhang, Q., Nie, Y., Wei, H., Wang, B., Huang, J., Yu, G., Xing, B., 2012. Sorption mechanisms of perfluorinated compounds on carbon nanotubes. Environ. Pollut. 168, 138–144.

Ding, G., Peijnenburg, W.J.G.M., 2013. Physicochemical properties and aquatic toxicity of poly- and perfluorinated compounds. Crit. Rev. Environ. Sci. Technol. 43 (6), 598–678.

Du, Z., Deng, S., Bei, Y., Huang, Q., Wang, B., Huang, J., Yu, G., 2014. Adsorption behavior and mechanism of perfluorinated compounds on various adsorbents-a review. J. Hazard. Mater. 274, 443–454.

Du, Z., Deng, S., Zhang, S., Wang, W., Wang, B., Huang, J., Wang, Y., Yu, G., Xing, B., 2017. Selective and fast adsorption of perfluorooctanesulfonate from wastewater by magnetic fluorinated vermiculite. Environ. Sci. Technol. 51 (14), 8027–8035.

Dzombak, D.A., Morel, F.M.M., 1990. Surface Complexation Modeling: Hydrous Ferric Oxide. John Wiley & Sons, New York.

European Union, 1999. Council directive/31/EC of 26 April 1999 on the landfill ofwaste. Off. J. Eur. Communities 26.

Fabregat-Palau, J., Vidal, M., Rigol, A., 2021. Modelling the sorption behaviour of perfluoroalkyl carboxylates and perfluoroalkane sulfonates in soils. Sci. Total Environ. 801, 149343.

Filella, M., Belzile, N., Chen, Y.W., 2002. Antimony in the environment: a review focused on natural waters II. Relevant solution chemistry. Earth Sci. Rev. 59 (1–4), 265–285.

Ghosh, U., Luthy, R.G., Cornelissen, G., Werner, D., Menzie, C.A., 2011. In-situ sorbent amendments: a new direction in contaminated sediment management. Environ. Sci. Technol. 45 (4), 1163–1168.

Gustafsson, O., Bucheli, T.D., Kukulska, Z., Andersson, M., Largeau, C., Rouzaud, J.N., Reddy, C.M., Eglinton, T.I., 2001. Evaluation of a protocol for the quantification of black carbon in sediments. Glob. Biogeochem. Cycles 15 (4), 881–890.

Hale, S.E., Cornelissen, G., Werner, D., 2009. Sorption of dichlorodiphenyltrichloroethane (DDT) and its metabolites by activated carbon in clean water and sediment slurries. Water Res. 43 (17), 4336–4346.

Hale, S.E., Arp, H.P.H., Slinde, G.A., Wade, E.J., Bjorseth, K., Breedveld, G.D., Straith, B.F., Moe, K.G., Jartun, M., Hoisaeter, A., 2017. Sorbent amendment as a remediation strategy to reduce PFAS mobility and leaching in a contaminated sandy soil from a norwegian firefighting training facility. Chemosphere 171, 9–18.

Heier, L.S., Lien, I.B., Stromseng, A.E., Ljones, M., Rosseland, B.O., Tollefsen, K.-E., Salbu, B., 2009. Speciation of lead, copper, zinc and antimony in water draining a shooting range-time dependant metal accumulation and biomarker responses in brown trout (Salmo trutta L.). Sci. Total Environ. 407 (13), 4047–4055.

Inyang, M., Dickenson, E., 2015. The potential role of biochar in the removal of organic and microbial contaminants from potable and reuse water: a review. Chemosphere 134, 232–240.

Johnson, V.G., Peterson, R.E., Olsen, K.B., 2005. Heavy metal transport and behavior in the lower Columbia River, USA. Environ. Monit. Assess. 110 (1–3), 271–289.

JRC, 2018. Status of local soil contamination in Europe. JRC Technical Reports EUR 29124 EN. EU Joint Research Centre (JRC).

Kim, M., Li, L.Y., Grace, J.R., Yue, C., 2015. Selecting reliable physicochemical properties of perfluoroalkyl and polyfluoroalkyl substances (PFASs) based on molecular descriptors. Environ. Pollut. 196, 462–472.

Kucharzyk, K.H., Darlington, R., Benotti, M., Deeb, R., Hawley, E., 2017. Novel treatment technologies for PFAS compounds: a critical review. J. Environ. Manag. 204, 757–764.

Kupryianchyk, D., Hale, S.E., Breedveld, G.D., Cornelissen, G., 2016. Treatment of sites contaminated with perfluorinated compounds using biochar amendment. Chemosphere 142, 35–40.

Kwon, S., Pignatello, J.J., 2005. Effect of natural organic substances on the surface and adsorptive properties of environmental black carbon (Char): pseudo pore blockage by model lipid components and its implications for N2-probed surface properties of natural sorbents. Environ. Sci. Technol. 39 (20), 7932–7939.

Leuz, A.K., Monch, H., Johnson, C.A., 2006. Sorption of Sb(III) and Sb(V) to goethite: influence on Sb(III) oxidation and mobilization. Environ. Sci. Technol. 40 (23), 727–728.

Lu, X., Deng, S., Wang, B., Huang, J., Wang, Y., Yu, G., 2016. Adsorption behavior and mechanism of perfluorooctane sulfonate on nanosized inorganic oxides. J. Colloid Interface Sci. 474, 199–205.

Mahinroosta, R., Senevirathna, L., 2020. A review of the emerging treatment technologies for PFAS contaminated soils. J. Environ. Manag. 255.

Martínez-Lladó, X., de Pablo, J., Giménez, J., Ayora, C., Martí, V., Rovira, M., 2008. Sorption of antimony (V) onto synthetic goethite in carbonate medium. Solvent Extr. Ion Exch. 26 (3), 289–300.

Miller, J. N. and J. C. Miller, n.d. Eds. Statistics and Chemometrics for Analytical Chemistry, Pearson Education Limited.

Milne, C.J., Kinniburgh, D.G., Van Riemsdijk, W.H., Tipping, E., 2003. Generic NICA-donnan model parameters for metal-ion binding by humic substances. Environ. Sci. Technol. 37 (5), 958–971.

Norwegian Ministry of Climate and Environment, 2004. Waste Regulation. FOR-2004-06-01-930.

O'Day, P.A., Vlassopoulos, D., 2010. Mineral-based amendments for remediation. Elements 6 (6), 375–381.

Okkenhaug, G., Amstätter, K., Lassen Bue, H., Cornelissen, G., Breedveld, G.D., Henriksen, T., Mulder, J., 2013. Antimony (Sb) contaminated shooting range soil: sb mobility and immobilization by soil amendments. Environ. Sci. Technol. 47 (12), 6431–6439.

Okkenhaug, G., Grasshorn Gebhardt, K.-A., Amstaetter, K., Lassen Bue, H., Herzel, H., Mariussen, E., Rossebø Almås, Å., Cornelissen, G., Breedveld, G.D., Rasmussen, G., Mulder, J., 2016. Antimony (Sb) and lead (Pb) in contaminated shooting range soils: sb and pb mobility and immobilization by iron based sorbents, a field study. J. Hazard. Mater. 307, 336–343.

Okkenhaug, G., Smebye, A.B., Pabst, T., Amundsen, C.E., Saevarsson, H., Breedveld, G.D., 2018. Shooting range contamination: mobility and transport of lead (Pb), copper (Cu) and antimony (Sb) in contaminated peatland. J. Soils Sediments 18 (11), 3310–3323.

Okkenhaug, G., Zhu, Y.-G., Luo, L., Lei, M., Li, X., Mulder, J., 2011. Distribution, speciation and availability of antimony (Sb) in soils and terrestrial plants from an active sb mining area. Environ. Pollut. 159 (10), 2427–2434.

Sarlaki, E., Sharif Paghaleh, A., Kianmehr, M.H., Asefpour Vakilian, K., 2021. Valorization of lignite wastes into humic acids: process optimization, energy efficiency and structural features analysis. Renew. Energy 163, 105–122.

Schwartz, Zhang, 2003. Fundamentals of Groundwater.

Schwarzenbach, R.P., Gschwend, P.M., Imboden, D.M., 2016. Environmental Organic Chemistry. John Wiley & Sons.

Silvani, L., Cornelissen, G., Botnen Smebye, A., Zhang, Y., Okkenhaug, G., Zimmerman, A.R., Thune, G., Saevarsson, H., Hale, S.E., 2019. Can biochar and designer biochar be used to remediate per- and polyfluorinated alkyl substances (PFAS) and lead and antimony contaminated soils? Sci. Total Environ. 694, 133693.

Sorengard, M., Kleja, D.B., Ahrens, L., 2019. Stabilization of per- and polyfluoroalkyl substances (PFASs) with colloidal activated carbon (PlumeStop(R)) as a function of soil clay and organic matter content. J. Environ. Manag. 249, 109345.

Sörengård, M., Östblom, E., Köhler, S., Ahrens, L., 2020. Adsorption behavior of per- and polyfluoralkyl substances (PFASs) to 44 inorganic and organic sorbents and use of dyes as proxies for PFAS sorption. J. Environ. Chem. Eng. 8 (3).

Sormo, E., Silvani, L., Bjerkli, N., Hagemann, N., Zimmerman, A.R., Hale, S.E., Hansen, C.B., Hartnik, T., Cornelissen, G., 2021. Stabilization of PFAS-contaminated soil with activated biochar. Sci. Total Environ. 763.

Sørmo, E., Silvani, L., Thune, G., Gerber, H., Schmidt, H.P., Smebye, A.B., Cornelissen, G., 2020. Waste timber pyrolysis in a medium-scale unit: emission budgets and biochar quality. Sci. Total Environ. 137335.

Trivedi, P., Dyer, J.A., Sparks, D.L., 2003. Lead sorption onto ferrihydrite. 1. A macroscopic and spectroscopic assessment. Environ. Sci. Technol. 37 (5), 908–914.

Vithanage, M., Rajapaksha, A.U., Ahmad, M., Uchimiya, M., Dou, X., Alessi, D.S., Ok, Y.S., 2015. Mechanisms of antimony adsorption onto soybean Stover-derived biochar in aqueous solutions. J. Environ. Manag. 151, 443–449.

Wang, W., Deng, S., Li, D., Ren, L., Shan, D., Wang, B., Huang, J., Wang, Y., Yu, G., 2018. Sorption behavior and mechanism of organophosphate flame retardants on activated carbons. Chem. Eng. J. 332, 286–292.

Wei, Y., Li, J., Shi, D., Liu, G., Zhao, Y., Shimaoka, T., 2017. Environmental challenges impeding the composting of biodegradable municipal solid waste: a critical review. Resour. Conserv. Recycl. 122, 51–65.

Xiao, X., Ulrich, B.A., Chen, B., Higgins, C.P., 2017. Sorption of poly-and perfluoroalkyl substances (PFASs) relevant to aqueous film-forming foam (AFFF)-impacted groundwater by biochars and activated carbon. Environ. Sci. Technol. 51 (11), 6342–6351.

Xu, X., Schierz, A., Xu, N., Cao, X., 2016. Comparison of the characteristics and mechanisms of hg (II) sorption by biochars and activated carbon. J. Colloid Interface Sci. 463, 55–60.

Zhang, Z., Wang, X., Wang, Y., Xia, S., Chen, L., Zhang, Y., Zhao, J., 2013. Pb(II) removal from water using fe-coated bamboo charcoal with the assistance of microwaves. J. Environ. Sci. 25 (5), 1044–1053.